

# A Momentum Interpolation Method for Laminar Incompressible Flows

N. Sreenivasalu Reddy<sup>1,\*</sup>, K. Rajagopal<sup>2</sup>, P.H. Veena<sup>3</sup>

<sup>1\*</sup>Department of Mechanical Engineering, RajaRajeswari College of Engineering, Bangalore, Karnataka, India, nsreddysrsit@gmail.com

<sup>2</sup>Department of Mechanical Engineering, JNTU College of Engineering, Hyderabad, Andhra Pradesh, India

<sup>3</sup>Department of Mathematics, Smt. V.G. College for Women, Gulberga, Karnataka, India

\*Corresponding author: E-mail address: nsreddysrsit@gmail.com

## ABSTRACT

A new analysis of the momentum interpolation method is presented in this paper. A modified method using quadratic interpolating polynomials for the calculation of the cell-face velocities is projected. The performance of the proposed method is examined and its application to lid-driven cavity problem is tested. The numerical results are compared with standard reported benchmark solutions for a different flow conditions. The numerical results show clearly the advantage of the new approach over the original momentum interpolation method, in terms of numerical accuracy, rate of convergence, and computational efficiency.

Keywords: staggered Grids, Collocated Grids, Finite Volume Method, SIMPLE method, lid driven cavity.

## 1. INTRODUCTION

In recent years, finite volume methods have become very popular for solving the incompressible Navier–Stokes equations. When scalar and vector variables (e.g. velocities and pressure) are used, special treatment is required in the solution algorithm and the grid system used. It is because of pressure does not have its own governing equation. The marker-and-cell (MAC) type staggered grid arrangement [1] of velocities and scalar variables, first proposed by Harlow and Welch [2], has been widely used with great success [3–6]. The main disadvantages of such an arrangement are the geometrical complexity (due to the different sets of grids used for different variables), the discretization complexity of the boundary conditions, and the difficulty of implementation to non-orthogonal curvilinear grids [7] and multigrid solution methods.

The pressure gradient terms, appearing in the momentum equations, are still represented by central difference approximation. Subsequent work by Peric [7] refined the original method further. Majumdar [10] and Miller and Schmidt [11] have removed the problem of underrelaxation parameter dependency of the results, observed in Rhie and Chow's formula. Previous authors have reported performance comparisons between the staggered and non-staggered grid arrangements [11–16].

In this paper, a new interpretation of the Momentum Interpolation Method (MIM) is provided. Based on this interpretation, it is shown that enhancements of the original method can be derived by using higher-order interpolating functions for the evaluation of the cell-face pseudo-velocities. Subsequently, a new formula based on quadratic interpolating polynomials is proposed. The same quadratic formula is also used for the representation of the pressure gradient terms. This results in a method of a greater formal accuracy that, at the same time, retains the basic characteristics of the momentum interpolation.

## 2. MATHEMATICAL FORMULATION

### 2.1 The Governing Equations

Consider a two-dimensional laminar viscous incompressible fluid flow and heat transfer in a Cartesian coordinate with non-constant properties. We have continuity equation

$$\frac{\partial(\rho u)}{\partial x} + \frac{\partial(\rho v)}{\partial y} = 0 \quad (1)$$

u-momentum equation

$$\frac{\partial(\rho u)}{\partial t} + \frac{\partial(\rho u u)}{\partial x} + \frac{\partial(\rho v u)}{\partial y} = -\frac{\partial p}{\partial x} + \frac{\partial}{\partial x} \left( \mu \frac{\partial u}{\partial x} \right) + \frac{\partial}{\partial y} \left( \mu \frac{\partial u}{\partial y} \right) + s_u \quad (2)$$

v-momentum equation

$$\frac{\partial(\rho v)}{\partial t} + \frac{\partial(\rho u v)}{\partial x} + \frac{\partial(\rho v v)}{\partial y} = -\frac{\partial p}{\partial y} + \frac{\partial}{\partial x} \left( \mu \frac{\partial v}{\partial x} \right) + \frac{\partial}{\partial y} \left( \mu \frac{\partial v}{\partial y} \right) + s_v \quad (3)$$

energy equation

$$\frac{\partial(\rho T)}{\partial t} + \frac{\partial(\rho u T)}{\partial x} + \frac{\partial(\rho v T)}{\partial y} = \frac{\partial}{\partial x} \left( k \frac{\partial T}{\partial x} \right) + \frac{\partial}{\partial y} \left( k \frac{\partial T}{\partial y} \right) + s_T \quad (4)$$

Equations (2) - (4) can be expressed in a general form:

$$\frac{\partial(\rho \Phi)}{\partial t} + \frac{\partial(\rho u \Phi)}{\partial x} + \frac{\partial(\rho v \Phi)}{\partial y} = \frac{\partial}{\partial x} \left( \Gamma \frac{\partial \Phi}{\partial x} \right) + \frac{\partial}{\partial y} \left( \Gamma \frac{\partial \Phi}{\partial y} \right) + s_\Phi \quad (5)$$

where  $u$  and  $v$  are the velocity in horizontal and vertical direction,  $\Phi$  is any dependent variable ( $u$ ,  $v$ , and  $T$ ), and  $t$ ,  $\rho$ ,  $\Gamma$ , and  $s_\Phi$  are time, density, diffusion coefficient, and source term, respectively. Note that for the continuity equation,  $\Phi = 1$ ,  $\Gamma = 0$ , and  $s_\Phi = 0$ . Integration of Equation (5) over the control volume-surrounding node  $P$  yields an algebraic equation representing the balance of fluxes. The resulting algebraic equations for the  $u$  velocity component at node  $P$  have the form

$$a_P|_P u_P = \sum_k a_k u_k|_P + b_P - A_P^x (P_e - P_w) \quad (6)$$

where  $a_k$ , is the convection and diffusion effects, depend on the discretization method used and the index  $k$  represents the four neighboring nodes of  $P$ . The  $b_P$  stands for the constant part of the discretized source term, which does not include the pressure gradient and  $A_P^x$  is a cross-sectional area at node  $P$ . The last term in the above equation represents the  $x$ -direction pressure driving force acting on the control volume. A similar equation can be obtained for the  $v$  velocity component.

The discretized form of the continuity equation is given by

$$\rho_e u_e A_e^x - \rho_w u_w A_w^x + \rho_n v_n A_n^y - \rho_s v_s A_s^y = 0 \quad (7)$$

Special care should be taken to the evaluation of cell-face velocities appearing in the continuity equation (7), and the cell-face pressure values appearing in the momentum equations (6), to avoid the velocity-pressure decoupling problem [1,8] and the subsequent non-physical oscillations in the pressure field.

## 2.2 Momentum interpolation method

Rhie and Chow [9] recommended the use of the same discretization equation for the cell-face velocities as for the nodal ones where all terms, with the exception of the pressure gradient, are obtained through linear interpolation of the corresponding terms in the equations for the neighboring cell-centered velocities. The pressure gradient term is not interpolated but replaced by the difference of pressure at the nodes between which the cell-face lies. This approach is known as the Momentum Interpolation Method (MIM). In a general, two-dimensional, non-uniform grid, the east face velocity, for example, is defined as follows:

$$u_e = \frac{\sum_k a_k u_k|_e}{a_P|_e} + \frac{b_e}{a_P|_e} - \frac{A_e^x}{a_P|_e} (P_E - P_P) \quad (8)$$

where

$$\frac{\sum_k a_k u_k|_e}{a_P|_e} = f_P^x \frac{\sum_k a_k u_k|_E}{a_P|_E} + (1 - f_P^x) \frac{\sum_k a_k u_k|_P}{a_P|_P} \quad (9)$$

$$\frac{b_e}{a_P|_e} = f_P^x \frac{b_e}{a_P|_E} + (1 - f_P^x) \frac{b_P}{a_P|_P} \quad (10)$$

$$\frac{1}{a_P|_e} = f_P^x \frac{1}{a_P|_E} + (1 - f_P^x) \frac{1}{a_P|_P} \quad (11)$$

and  $f_P^x$  is the  $x$ -direction linear interpolation factor, defined in terms of distances between nodes as

$$f_P^x = \frac{\overline{P_e}}{P_E} = \frac{x_e - x_P}{x_E - x_P} \quad (12)$$

The last term in Equation (8) represents the net pressure driving force acting on the 'staggered' control volume surrounding the east face. By substituting Equations (9) and (10) into Equation (8) and rearranging, the cell-face velocity can be expressed explicitly in terms of the known nodal velocities

$$u_c = f_p^x u_E + (1 - f_p^x) u_P + f_p^x \frac{A_E^x}{a_{p|E}} (P_E - P_P) + (1 - f_p^x) \frac{A_P^x}{a_{p|P}} (P_P - P_W) - \frac{A_c^x}{a_{p|c}} (P_E - P_P) \quad (13)$$

Similar expressions can be obtained for the other cell-face velocities  $u_w, v_n, v_s$ .

### 2.3 interpretation of momentum equation

The above expression (13) can be recast in a more compact format, which provides simplicity and clarity. First, the momentum equation (2) giving the nodal velocity  $u_p$  is rewritten in a more suitable form,

$$u_p = \hat{u}_p + \bar{u}_p \quad (14)$$

The first term on the right hand side of the equation (14) is a pseudo-velocity [1] composed of the neighboring velocities and containing no pressure terms,

$$\hat{u}_p = \frac{\sum_k a_k u_k|_p}{a_p|_p} + \frac{b_p}{a_p|_p}, \quad (15)$$

and the second term on the right hand side of the equation (14) is contribution of pressure to the actual value of velocity,

$$\bar{u}_p = -\frac{A_p^x}{a_p|_p} (P_e - P_w). \quad (16)$$

Using the above splitting formulation, Equation (8) can be recast into the following form:

$$u_c = \hat{u}_c + \bar{u}_c \quad (17)$$

where

$$\hat{u}_c = f_p^x \hat{u}_E + (1 - f_p^x) \hat{u}_P \quad (18)$$

and

$$\bar{u}_c = -\frac{A_c^x}{a_p|_c} (P_E - P_P). \quad (19)$$

The expression giving  $u_c$  (17) is made up of two parts. The first part, representing the cell-face pseudo-velocity, is approximated by a linear interpolation of the neighboring cell-centered pseudo-velocities. The second part stands for the contribution of pressure and is evaluated by the pressure difference acting on the ‘staggered’ control volume surrounding  $u_c$ . The need for more accurate results, especially on coarse grids, makes a further effort in improving the MIM necessary, i.e. in the use of a more accurate interpolation practice for the evaluation of the cell-face pseudo-velocities.

### 2.4 new momentum interpolation method

The general form of the quadratic interpolation formula has been presented by Arambatzis *et al.* [18] in their formulation of the QUICK scheme. According to this formulation, the formulae giving the general transport quantity  $\phi$  at the east and north cell-faces for a two-dimensional flow have the following form

$$\begin{aligned} \phi_e &= Q_e(\phi) \\ &= \begin{cases} \phi_P + QAE_P(\phi_P - \phi_W) + QBE_P(\phi_E - \phi_P) + QC_P(\phi_S - \phi_P) + QD_P(\phi_N - \phi_P) & u_e \geq 0 \\ \phi_E + QAW_E(\phi_P - \phi_E) + QBW_E(\phi_E - \phi_{EE}) + QC_E(\phi_{SE} - \phi_E) + QDE(\phi_{NE} - \phi_E) & u_e < 0 \end{cases} \end{aligned} \quad (20)$$

$$\begin{aligned} \phi_n &= Q_n(\phi) \\ &= \begin{cases} \phi_P + QCN_P(\phi_P - \phi_S) + QDN_P(\phi_N - \phi_P) + QA_P(\phi_W - \phi_P) + QB_P(\phi_E - \phi_P) & v_n \geq 0 \\ \phi_N + QCS_N(\phi_P - \phi_N) + QDS_N(\phi_N - \phi_{NN}) + QA_N(\phi_{NW} - \phi_N) + QB_N(\phi_{NE} - \phi_N) & v_n < 0 \end{cases} \end{aligned} \quad (21)$$

Where the coefficients QAE<sub>p</sub>, QBE<sub>p</sub>, etc., are functions of the distances between nodes. The above formulae, representing the face averages of the quantity  $\phi$ , are derived by fitting a parabola to the nodal values and integrating along the cell-faces. Using the above formulae for the evaluation of cell-face pseudo-velocities, the expressions giving the east face velocity can be written as

$$u_c = Q_c(\hat{u}) + \bar{u}_c \quad (22)$$

Equation (22) can be expressed in the following in the following computationally efficient form, using the cell-centered momentum equations (15):

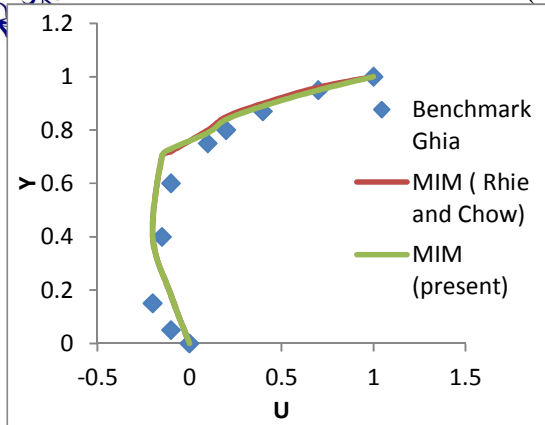


Figure 1. Horizontal velocity profile along cavity centerline,  $Re = 100$

$$u_e = Q_e(u) + \bar{u}_e - Q_e(\bar{u}). \quad (23)$$

This expression does not contain pseudo-velocities but velocity and pressure values, and can be used immediately to compute  $u_e^*$ , requiring no extra storage. A similar expression can be obtained for the north face velocity

$$v_n = Q_n(v) + \bar{v}_n - Q_n(\bar{v}). \quad (24)$$

The proposed interpolation is more appropriate when used in combination with the QUICK differencing scheme, where the convected cell-face velocities are approximated to third-order by formulae (20) and (21), setting  $\phi = u$  or  $v$ . The Rhie and Chow momentum interpolation of the convecting cell-face velocities is of only second-order (the order of linear interpolation, see Miller and Schmidt [11]). In the new momentum interpolation scheme, the convecting cell-face velocities are approximated to third-order by formulae (23) and (6), giving overall third-order accuracy to the finite difference equations.

### 2.5. Evaluation of cell-face pressures

In order to preserve overall consistency in an algorithm using the quadratic momentum interpolation practice, it is reasonable to adopt the same interpolation method when calculating the pressure values at the cell faces. These values are needed for the evaluation of the correction part of cell-face velocities according to the above interpolation practice, and also for the calculation of the pressure gradient source term in the momentum

equations. The interpolation equations used are (20) and (21), where  $\phi = p$

### 2.6. Implementation of MIM in SIMPLE (Semi Implicit Method for pressure Linked Equations)

In the present study, the SIMPLE algorithm treats the coupling between the continuity and the momentum equation. In the first step of SIMPLE, the pressure field from a previous iteration  $P^*$  determines a tentative velocity field  $u^*$ . To get a converged solution, these starred fields have to be corrected by pressure and velocity corrections  $P'$ ,  $u'$ .

## 3.0 RESULTS AND DISCUSSION

### 3.1. The test problem

The proposed new MIM is applied to the well-known lid-driven square cavity problem, in order to validate the calculation procedure as well as to assess its performance relative to Rhie and Chow's interpolation method. Because of simple geometry this case has been served as a standard benchmark problem for the evaluation of new algorithms. The problem is solved for Reynolds numbers ranging from 100 to 5000. The Reynolds number is defined by  $Re = \rho UL/\mu$ , where  $L$  is the length of the cavity and  $U$  is the velocity of the sliding wall. The QUICK differencing scheme of Leonard [17], as presented in Reference [18], is used for the discretization of the convective terms and the algebraic equations are solved by the strongly implicit procedure (SIP) [20]

### 3.2. The effect of Reynolds number

Figures 1–3 show the comparison of the horizontal velocity profiles along the vertical cavity centerline ( $x/L = 0.5$ ) for Reynolds numbers 100, 1000 and 5000. Each figure provides a comparison between the original MIM and the new MIM. Also, the results calculated by Ghia *et al.* [19] are shown. All the results presented in this section are obtained on a coarse, uniformly spaced grid consisting of  $15 \times 15$  nodes (13 internal control volumes in each direction). The comparisons clearly show the superior accuracy of the new MIM. The profiles plotted in Figure 1, for  $Re = 100$ , show that the results obtained by the new MIM are in closer agreement with the benchmark solution. As the Reynolds number increases (Figures 2 and 3), the differences between the two methods with respect to the benchmark results become more significant. This indicates that, at higher Reynolds numbers, the approximations adopted for the evaluation of cell-face pseudo-velocities and the cell-face pressures have significantly more influence on the accuracy of the final solution. This is the desirable behavior of the new method making it

suitable for high-Reynolds numbers simulations. Profiles of the vertical velocity  $v$  along the horizontal cavity centerline ( $y/L = 0.5$ ) are shown in Figures 4, 5 and 6 for Reynolds numbers 100, 1000 and 5000. The same observations as before can be made.

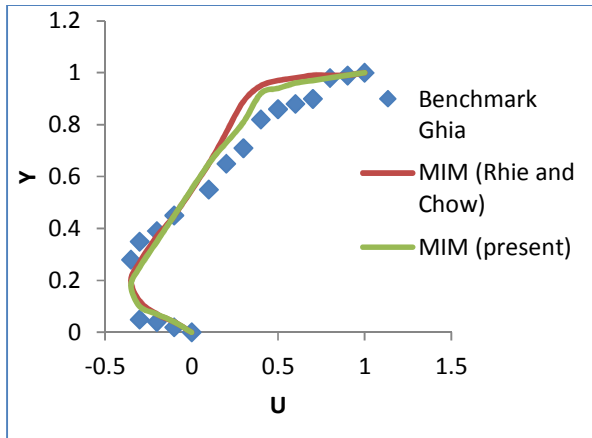


Figure 2. Horizontal velocity profile along cavity centerline,  $Re = 100$

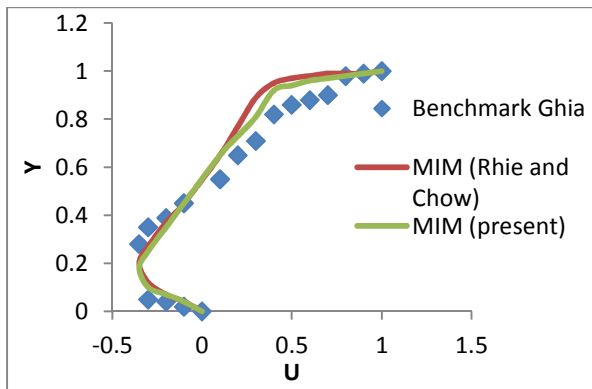


Figure 3. Horizontal velocity profile along cavity centerline,  $Re = 5000$

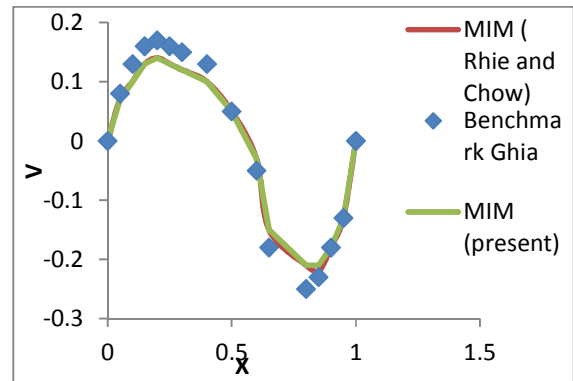


Figure 4. Vertical velocity profile along cavity centerline,  $Re = 100$ .

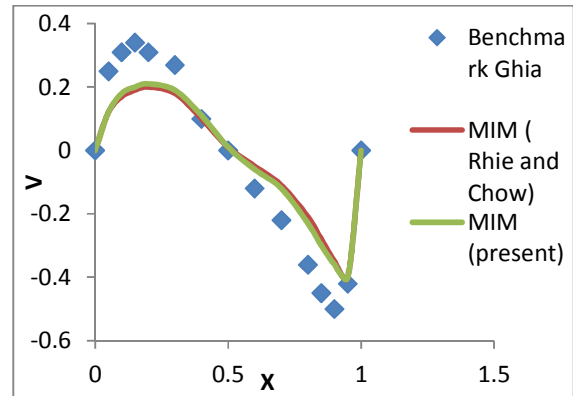


Figure 5. Vertical velocity profile along cavity centerline,  $Re = 1000$ .

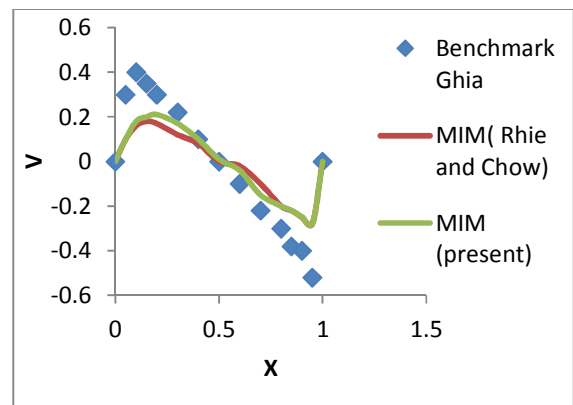


Figure 6. Vertical velocity profile along cavity centerline,  $Re = 5000$

#### 4. CONCLUSIONS

- In this paper it is shown that the discretized momentum equations for the cell-face velocities are composed of two parts. A velocity part calculated by the interpolation of the neighboring velocities, and a pressure driving force term on the 'staggered' control volume.
- The proposed new method, which uses higher order interpolation formulae to determine the cell-face velocities. New compact and computationally efficient expressions, containing no pseudo velocities have been derived in order to be used in computer codes.
- Cell face pressures were also calculated by the same interpolation formulae in order to maintain overall consistency in the new method. Finally, the implementation of QMIM in the SIMPLE algorithm has been described.
- The proposed new MIM has been found to give more accurate results than the original MIM (Rhie and Chow). The difference between the two methods increases as the Reynolds number increases in the lid-driven cavity benchmark problem.

#### REFERENCES

1. Patankar SV. *Numerical Heat Transfer and Fluid Flow*. Hemisphere: New York, 1980.
2. Harlow FH, Welch JE. Numerical calculation of time-dependent viscous incompressible flow of fluid with free surface. *The Physics of Fluids* 1965; **8**: 2182–2189.
3. Patankar SV, Spalding DB. A calculation procedure for heat, mass and momentum transfer in three-dimensional parabolic flows. *International Journal for Heat and Mass Transfer* 1972; **15**: 1787–1806.
4. Van Doormal JP, Raithby GD. Enhancement of the SIMPLE method for predicting incompressible fluid flows. *Numerical Heat Transfer* 1984; **7**: 147–163.
5. Markatos NC, Pericleous KK, Simitovic R. A hydrometeorological, three-dimensional model of thermal energy releases into environmental media. *International Journal for Numerical Methods in Fluids* 1987; **7**: 263–276.
6. Barakos G, Mitsoulis E, Assimacopoulos D. Natural convection flow in square cavity revised: laminar and turbulent models with wall functions. *International Journal for Numerical Methods in Fluids* 1994; **18**: 695–719.
7. Peric M. A finite volume method for the prediction of three-dimensional fluid flow in complex ducts. PhD Thesis, University of London, 1985.
8. Date AW. Solution of Navier–Stokes equations on non-staggered grid. *International Journal for Heat and Mass Transfer* 1993; **36**: 1913–1922.
9. separation. *AIAA Journal* 1983; **21**: 1525–1532.
10. Majumdar S. Role of underrelaxation in momentum interpolation for calculation of flow with non-staggered grids. *Numerical Heat Transfer* 1988; **13**: 125–132.
11. Miller TF, Schmidt FW. Use of a pressure-weighted interpolation method for the solution of the incompressible Navier–Stokes equations on a non-staggered grid system. *Numerical Heat Transfer* 1988; **14**: 213–233.
12. Aksoy H, Chen C-J. Numerical solution of Navier–Stokes equations with non-staggered grids. *Numerical Heat Transfer B* 1992; **21**: 287–306.
13. Melaen MC. Calculation of fluid flows with staggered and non-staggered curvilinear non-orthogonal grids—the theory. *Numerical Heat Transfer B* 1992; **21**: 1–19.
14. Melaen MC. Calculation of fluid flows with staggered and non-staggered curvilinear non-orthogonal grids—a comparison. *Numerical Heat Transfer B* 1992; **21**: 21–39.
15. Choi SK, Yun Nam H, Cho M. Use of staggered and nonstaggered grid arrangements for incompressible flow calculations on nonorthogonal grids. *Numerical Heat Transfer B* 1994; **25**: 193–204.
16. Choi SK, Nam HY, Cho M. Systematic comparison of finite volume methods with staggered and non-staggered grid arrangements. *Numerical Heat Transfer B* 1994; **25**: 205–221. Copyright © 2000 John Wiley & Sons, Ltd. *Int. J. Numer*
17. Leonard BP. A stable accurate convective modelling procedure based on quadratic upstream interpolation. *Computational Methods in Applied Mechanical Engineering* 1979; **19**: 59–98.
18. Arampatzis G, Assimacopoulos D, Mitsoulis E. Treatment of numerical diffusion in strong convective flows. *International Journal for Numerical Methods in Fluids* 1994; **18**: 313–331.
19. Ghia U, Ghia KN, Shin CT. High-*Re* solutions for incompressible flow using the Navier–Stokes equations and a multigrid method. *Journal of Computational Physics* 1982; **48**: 387–411.
20. Stone HL. Iterative solution of implicit approximation of multidimensional partial differential equations. *SIAM Journal of Numerical Analysis* 1968; **5**: 530–558. Copyright